Electronic Supplementary Material (ESI) for RSC Advances.

Theoretical study on photophysical properties of boron-fused double helicenes

Yanling Si,[*a] Yan Cheng,[b] Nan Qu,[a] Xinyu Zhao,[a] and Guochun Yang[*c]

a. College of Resource and Environmental Science, Jilin Agricultural University, Changchun 130118, China

b. Department of Ophthalmology, Second Hospital of Jilin University, Changchun, 132400, China

c. Centre for Advanced Optoelectronic Functional Materials Research and Key Laboratory for UV Light-Emitting Materials and Technology of Ministry of Education, Northeast Normal University, Changchun 130024, China

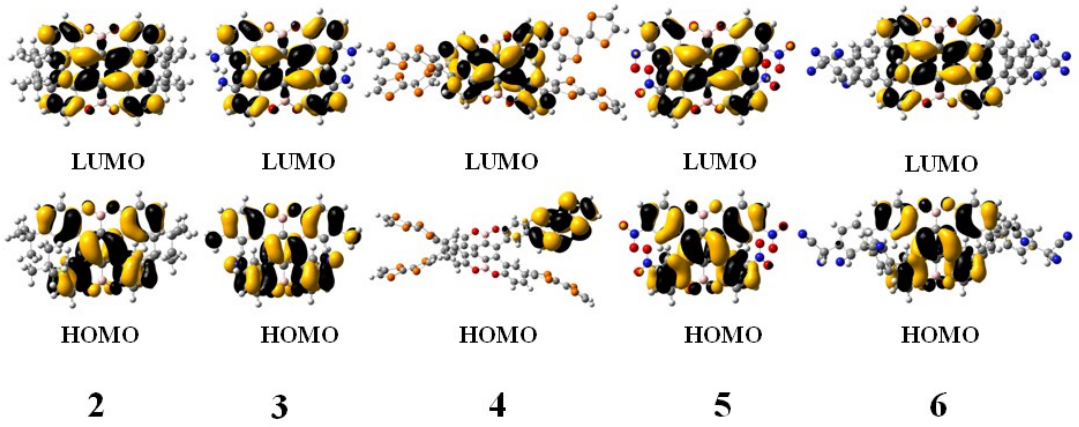

Fig. S1 HOMO and LUMO of compounds **2-6**.

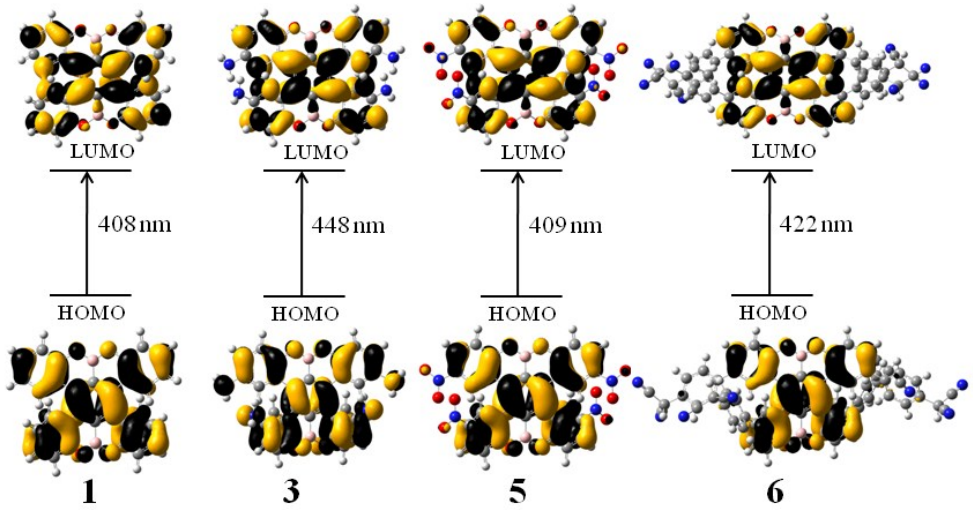

Fig. S2 Molecular orbital isosurfaces involved in the main electron transitions of compounds **1**, **3**, **5** and **6**.

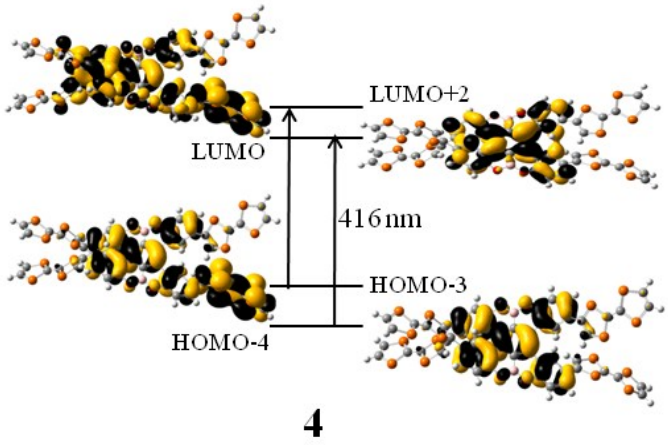

Fig. S3 Molecular orbital isosurfaces involved in the main electron transitions of compound **4**.

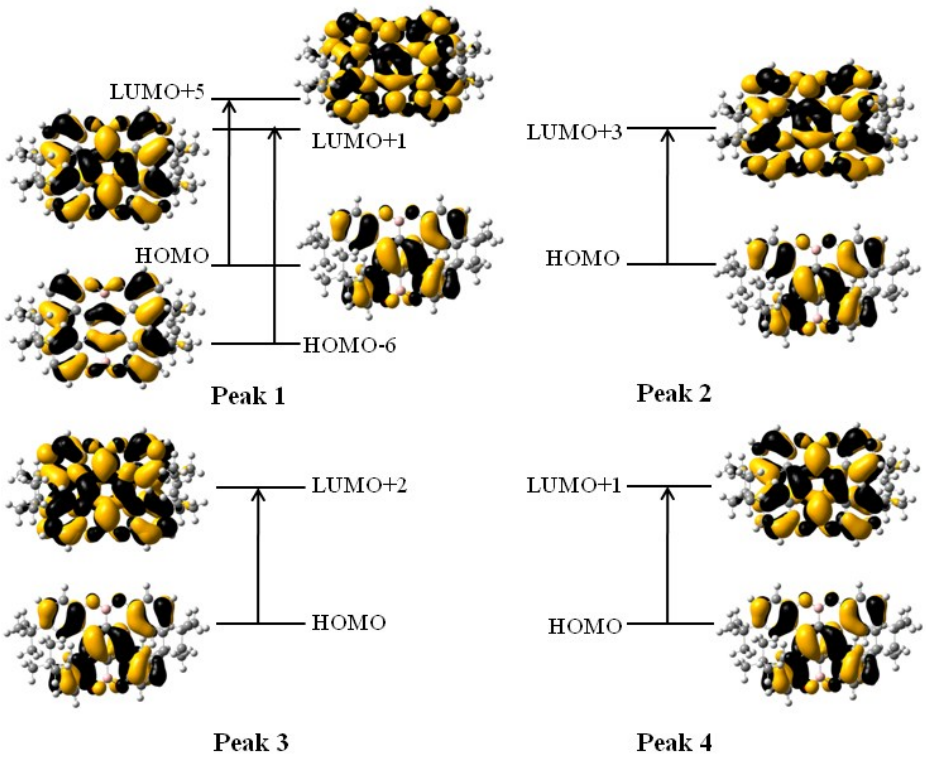

Fig. S4 Molecular orbitals involved into the main ECD transitions of compound **2**.

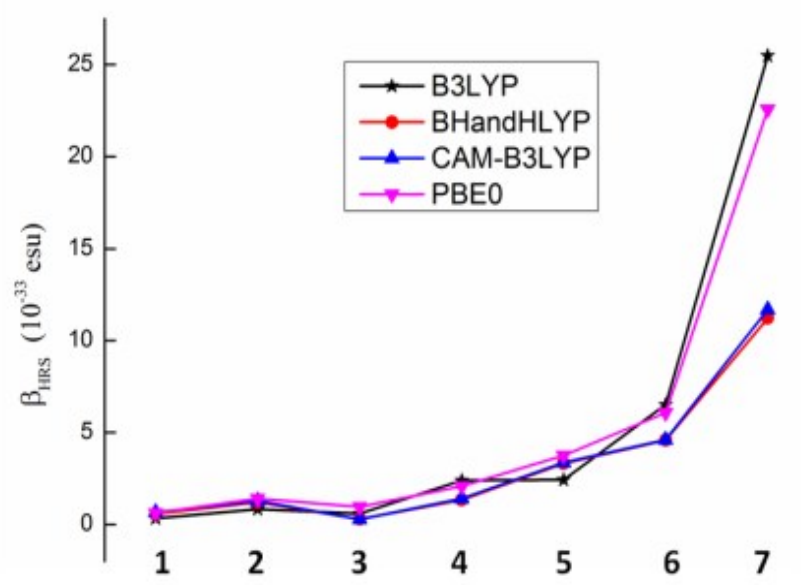

Fig. S5 The calculated second-order NLO response values obtained from the four functionals (i.e. B3LYP, BHandHLYP, CAM-B3LYP and PBE0).

Table S1. Calculated absorption wavelength (nm) for compound **2** with the TDDFT method at the PBE0, B3LYP, Cam-B3LYP and BHandHLYP level, respectively, together with the experimental data.

λ_{cal} PBE0	λ_{cal} B3LYP	λ_{cal} Cam-B3LYP	λ_{cal} BHandHLYP	Exp.[20]
415	432	382	383	411

Table S2. The main concerned bond lengths and dihedral angles for compound **1** obtained by B3LYP and PBE0.

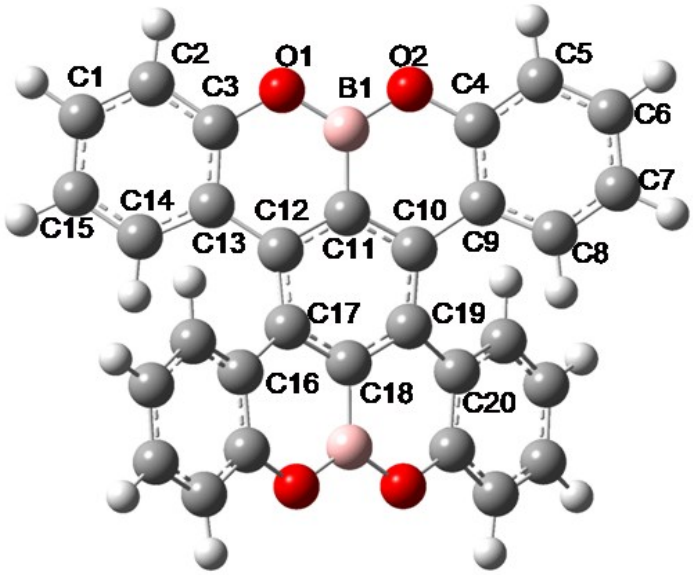

	Experiment[20]	B3LYP	PBE0	[a]Di(B3LYP)	[a]Di(PBE0)
Bond lengths				0.006[b]	0.006[b]
C1-C2	1.380	1.389	1.385	0.009	0.005
C2-C3	1.388	1.397	1.394	0.009	0.006
C3-O1	1.384	1.371	1.362	-0.013	-0.022
O1-B1	1.371	1.370	1.367	-0.001	-0.004
B1-O2	1.371	1.370	1.367	-0.001	-0.004
O2-C4	1.384	1.371	1.362	-0.013	-0.022
C4-C5	1.388	1.397	1.394	0.009	0.006
C5-C6	1.380	1.389	1.385	0.009	0.005
C6-C7	1.390	1.399	1.396	0.009	0.006
C7-C8	1.379	1.388	1.384	0.009	0.005
C8-C9	1.408	1.412	1.408	0.004	0.000
C9-C10	1.476	1.477	1.471	0.001	-0.005
C10-C11	1.411	1.415	1.410	0.004	-0.001
C11-C12	1.410	1.415	1.410	0.005	0.000
C12-C13	1.476	1.477	1.471	0.001	-0.005
C13-C14	1.411	1.412	1.408	0.001	-0.003
C14-C15	1.381	1.388	1.384	0.007	0.003
C12-C17	1.424	1.425	1.420	0.001	-0.004
C10-C19	1.418	1.425	1.420	0.007	0.002

Dihedral angles				0.72[b]	0.72[b]
C15-C14-C13-C12	-177.8	-177.5	-177.6	0.30	0.20
C13-C12-C17-C16	-29.1	-30.1	-29.5	-1.0	-0.4
C11-C12-C17-C16	153.1	152.7	153.2	-0.4	0.1
C7-C8-C9-C10	-177.8	-177.5	-177.6	0.3	0.2
C9-C10-C19-C20	-31.3	-30.1	-29.5	1.2	1.8
C9-C10-C19-C18	151.6	152.7	153.2	1.1	1.6

Note: [a] Difference is equal to calculation value minus experimental one; [b] the average deviation.

Table S3. The calculated excitation energies, oscillator strengths and rotational strengths for compound **1** in the gas phase at the TD-B3LYP/ 6-31+G(d) level.

states	eV	λ[a]	*f* [b]	R(length)[c]	R(velocity)[c]
1	3.0374	408.20	0.3137	-22.9109	-22.8690
2	3.3320	372.10	0.1326	-10.9780	-11.1988
3	3.9441	314.36	0.0088	-11.6785	-13.8186
4	3.9790	311.59	0.0000	0.0000	0.0000
5	4.1287	300.30	0.7960	38.7235	37.6812
6	4.1541	298.46	0.0290	45.4575	44.8711
7	4.1784	296.72	0.0685	-269.3065	-269.0754
8	4.2363	292.67	0.0037	4.7657	4.4278
9	4.3409	285.62	0.0747	58.7928	58.8044
10	4.4194	280.54	0.0039	-37.6095	-37.6775
11	4.4242	280.24	0.0056	-6.2162	-6.0301
12	4.6016	269.44	0.0003	1.9994	1.8345
13	4.6578	266.19	0.0028	98.2963	83.7974
14	4.6594	266.09	0.0000	0.0011	0.0009
15	4.6696	265.52	0.0105	-39.8177	-33.9864
16	4.6867	264.55	0.0000	0.0000	0.0000
17	4.7052	263.50	0.0040	-3.8650	-3.5139
18	4.8342	256.47	0.0000	0.0000	0.0000
19	4.8912	253.48	0.1312	-15.7621	-15.6281
20	4.9634	249.80	0.0470	67.7661	64.8276
21	5.0685	244.62	0.0000	0.0000	0.0000
22	5.2153	237.73	0.0102	7.7090	7.5944
23	5.2579	235.80	0.0100	-5.3824	-5.0732
24	5.2908	234.34	0.0000	0.0000	0.0000
25	5.3395	232.20	0.0046	-118.3632	-119.6333
26	5.3672	231.00	0.0366	71.9733	67.2055
27	5.4286	228.39	0.0000	0.0000	0.0000
28	5.4674	226.77	0.0027	2.5120	2.1097
29	5.4953	225.62	0.0000	0.0000	0.0000

30	5.5227	224.50	0.0112	-0.8186	-0.8171
31	5.5630	222.87	0.0000	0.0000	0.0000
32	5.6023	221.31	0.0822	19.4237	19.3428
33	5.6304	220.20	0.0057	-9.4311	-9.0675
34	5.6474	219.54	0.0000	-0.0003	-0.0003
35	5.6980	217.59	0.1016	-351.1712	-341.7341
36	5.7143	216.97	0.0020	14.3071	13.2134
37	5.7566	215.38	0.1350	80.8398	79.2522
38	5.7974	213.86	0.0318	47.9891	46.7837
39	5.8170	213.14	0.0045	14.8833	14.9468
40	5.8474	212.03	0.0002	-0.0248	-0.0245
41	5.8476	212.03	0.1030	-15.5834	-15.4300
42	5.8555	211.74	0.4788	224.4538	220.1685
43	5.8865	210.62	0.1509	-99.4823	-97.4308
44	5.8940	210.36	0.0116	93.9044	90.0693
45	5.9098	209.80	0.0405	-36.0440	-34.6405
46	5.9117	209.73	0.0000	-0.0006	-0.0006
47	5.9380	208.80	0.0168	-0.2442	-0.2262
48	5.9785	207.38	0.0000	0.0001	0.0001
49	5.9868	207.10	0.0005	-3.0361	-2.8093
50	6.0026	206.55	0.0968	-21.5322	-20.5613
51	6.0036	206.52	0.2323	221.9836	214.0286
52	6.0328	205.52	0.0057	5.2569	4.8050
53	6.0695	204.27	0.0233	-229.5323	-230.5940
54	6.0733	204.15	0.0528	-3.7735	-3.5810
55	6.1231	202.49	0.0000	-0.0003	-0.0003
56	6.1337	202.14	0.0014	0.1632	0.1369
57	6.1651	201.11	0.0000	-0.0001	-0.0001
58	6.1784	200.67	0.0376	-23.7002	-22.6825
59	6.1835	200.51	0.0599	-63.5343	-60.6609
60	6.1889	200.33	0.0173	-141.3005	-136.1755
61	6.2014	199.93	0.0218	8.0098	8.3552
62	6.2168	199.43	0.0435	15.1027	15.3735
63	6.2328	198.92	0.0105	-58.3597	-58.3838
64	6.2441	198.56	0.0000	0.0012	0.0012
65	6.2473	198.46	0.0288	24.8104	23.3321
66	6.2513	198.33	0.0015	26.4011	27.9903
67	6.2567	198.16	0.0329	-48.4204	-45.4358
68	6.2645	197.92	0.0294	26.3704	24.9460
69	6.2753	197.57	0.0379	73.3035	68.9831
70	6.2944	196.97	0.0000	0.0003	0.0003
71	6.3122	196.42	0.0042	-33.5558	-30.6976
72	6.3428	195.47	0.0062	3.8766	4.0130
73	6.3538	195.13	0.0000	-0.0059	-0.0057
74	6.3600	194.94	0.0435	-51.5035	-49.2530
75	6.3625	194.87	0.5633	-40.1803	-39.6041
76	6.3739	194.52	0.0070	-18.6825	-18.2100
77	6.4018	193.67	0.1777	174.1860	171.7646
78	6.4131	193.33	0.0000	-0.2582	-1.0337

79	6.4221	193.06	0.0065	-9.2991	-8.0907
80	6.4243	192.99	0.0025	18.3082	14.7613
81	6.4419	192.47	0.0783	-90.2354	-91.2010
82	6.4664	191.74	0.0000	-0.0001	-0.0001
83	6.4757	191.46	0.0506	12.6260	12.3388
84	6.4812	191.30	0.0244	37.8173	38.2368
85	6.5042	190.62	0.0000	0.0000	0.0000
86	6.5294	189.88	0.0000	0.0000	0.0000
87	6.5378	189.64	0.0000	0.0000	0.0000
88	6.5687	188.75	0.0149	-16.6698	-15.8300
89	6.5721	188.65	0.0044	-30.6836	-27.7350
90	6.5823	188.36	0.0756	154.4205	154.5330
91	6.6153	187.42	0.0070	12.0308	12.1214
92	6.6274	187.08	0.0000	0.0000	0.0000
93	6.6361	186.83	0.0764	-26.8702	-26.5477
94	6.6379	186.78	0.0111	21.2082	20.1858
95	6.6401	186.72	0.0000	-0.0701	-0.0665
96	6.6407	186.70	0.0040	-91.0725	-86.2831
97	6.6545	186.32	0.0764	43.7191	42.8066
98	6.6587	186.20	0.0024	-2.9533	-2.7341
99	6.6887	185.36	0.0000	0.0000	0.0000
100	6.6984	185.09	0.0122	-7.6319	-6.9513

[a]λ in nm. [b]Oscillator Strengths. [c]R values (in 10^{-40} esu^2cm^2) using the velocity-gauge representation and length-gauge representation of the electric dipole operator.